

## Research Article

# Urea-Based Synthesis of Zinc Oxide Nanostructures at Low Temperature

J. Z. Marinho,<sup>1</sup> F. C. Romeiro,<sup>1</sup> S. C. S. Lemos,<sup>1</sup> F. V. Motta,<sup>2</sup>  
C. S. Riccardi,<sup>3</sup> M. S. Li,<sup>4</sup> E. Longo,<sup>3</sup> and R. C. Lima<sup>1</sup>

<sup>1</sup>Instituto de Química, Universidade Federal de Uberlândia, 38400-902 Uberlândia, MG, Brazil

<sup>2</sup>Departamento de Engenharia de Materiais, Universidade Federal do Rio Grande do Norte, 59072-970 Natal, RN, Brazil

<sup>3</sup>Instituto de Química, Universidade Estadual Paulista, 14800-900 Araraquara, SP, Brazil

<sup>4</sup>Instituto de Física de São Carlos, Universidade de São Paulo, 13566-590 São Carlos, SP, Brazil

Correspondence should be addressed to R. C. Lima, rclima@iqufu.ufu.br

Received 17 December 2011; Revised 29 February 2012; Accepted 15 March 2012

Academic Editor: Laécio Santos Cavalcante

Copyright © 2012 J. Z. Marinho et al. This is an open access article distributed under the Creative Commons Attribution License, which permits unrestricted use, distribution, and reproduction in any medium, provided the original work is properly cited.

The preparation of nanometer-sized structures of zinc oxide (ZnO) from zinc acetate and urea as raw materials was performed using conventional water bath heating and a microwave hydrothermal (MH) method in an aqueous solution. The oxide formation is controlled by decomposition of the added urea in the sealed autoclave. The influence of urea and the synthesis method on the final product formation are discussed. Broadband photoluminescence (PL) behavior in visible-range spectra was observed with a maximum peak centered in the green region which was attributed to different defects and the structural changes involved with ZnO crystals which were produced during the nucleation process.

## 1. Introduction

Zinc oxide (ZnO) is a well-known semiconducting material with photoluminescent and electric conductivity which has a band gap value of 3.37 eV and an excitation energy band of 60 meV at room temperature [1, 2]. With these properties, ZnO has a wide area of application such as solar cells [3, 4], catalysis [5, 6], sensors [7], laser diodes [8], and varistors [5, 9]. Chemical and structural properties of ZnO particles are very important in these applications; different preparation methods for this oxide were used by various researchers such as a sol-gel process [10], homogeneous precipitation [5], thermal decomposition [11], microwave heating [12], a conventional hydrothermal method [13–17], a polymeric precursor method [10], and an MH-assisted method [18, 19]. The characteristics of the powders obtained for specific applications are determined by the crystal size, morphology, porosity, crystal type, and particle shape [6, 20, 21].

The use of polymers or surfactants [22, 23] to prepare zinc oxide nanoparticles is advantageous due to a surface modification process which eliminates agglomeration during

synthesis and controls the morphology and the shape of developed ZnO nanocrystals. However, repetitive washing and centrifugation is required with appropriate reagents such as absolute ethanol and distilled water. Therefore, directly controlling experimental factors to obtain nanoparticles with ideal morphologies is a significant objective which is essential for future device application [24]. Furthermore, the MH method has commanded intensive interest due to simple manipulation, low cost, clean technology, and short synthesis time [25–27].

In this paper, the effect of the synthesis method on the formation of zinc oxide nanostructures in an aqueous solution was investigated. Thus, we prepared this oxide using conventional water bath heating and the MH method using urea as one of the reactants. The samples were characterized by field emission gun scanning electron microscopy (FE-SEM) and Raman spectroscopy. The formation of a hexagonal ZnO wurtzite phase was verified by X-ray diffraction (XRD) patterns. The morphology, growth mechanism, and PL properties were recorded.

## 2. Experimental

**2.1. Synthesis.** Zinc oxide nanostructures were obtained: zinc acetate ( $\text{Zn}(\text{CH}_3\text{COO})_2 \cdot 2\text{H}_2\text{O}$ ) (99%, Aldrich) and urea ( $\text{CO}(\text{NH}_2)_2$ ) (99%, Synth) (1:1 stoichiometry) were dissolved in deionized water under constant agitation. A potassium hydroxide (KOH) (3.0 mol/L solution) was added until the pH reached 12 followed by stirring at room temperature for 15 min.

The solution was then heated by two different methods: conventional water bath heating and the MH method. In the MH heating, the solution was transferred to a Teflon-lined stainless steel autoclave, sealed, and placed in domestic microwave (2.45 GHz) which was maintained at  $100^\circ\text{C}$  for 2 and 8 min. The pressure in the sealed autoclave was stabilized at 1.0 atm. The autoclave was cooled to room temperature naturally. A white product was separated by centrifugation, washed with deionized water and ethanol, and dried at  $60^\circ\text{C}$  in air.

**2.2. Characterization of Samples.** The powders obtained were structurally characterized by XRD using a Shimadzu XRD 6000 (Japan) equipped with  $\text{CuK}\alpha$  radiation ( $\lambda = 1.5406 \text{ \AA}$ ) in the  $2\theta$  range from  $10^\circ$  to  $80^\circ$  with  $0.02^\circ/\text{min}$  scan increment. The morphology was characterized by FE-SEM (Supra 35-VP, Carl Zeiss, Germany). Raman spectra were recorded on a RFS/100/S Bruker FT-Raman spectrometer with a Nd:YAG laser providing an excitation light at  $1064.0 \text{ nm}$  and a spectral resolution of  $4 \text{ cm}^{-1}$ . The PL was measured with a Thermal Jarrel-Ash Monospec 27 monochromator and a Hamamatsu R446 photomultiplier. The  $350.7 \text{ nm}$  exciting wavelength of a krypton ion laser (Coherent Innova) was employed, and the nominal output power of the laser was maintained at  $550 \text{ mW}$ . All measurements were made at room temperature.

## 3. Results and Discussion

XRD patterns of samples obtained using conventional water bath heating and the MH method for 2 and 8 min are shown in Figure 1. The results revealed that all diffraction peaks can be indexed to the hexagonal ZnO structure which shows good agreement with data reported in the literature (JCPDS card number 36-1451). The strong and sharp peaks indicate that the zinc oxide powders are highly crystalline and structurally ordered at long range. These results show that the MH processing promotes the complete crystallization of ZnO samples at low temperatures and reduced processing time. No secondary phases were detected.

Five active Raman modes can be observed for ZnO samples: (i) at  $437 \text{ cm}^{-1}$  a narrow strong band has been assigned to one of the two  $E_2$  modes involving mainly a Zn motion which is a band characteristic of the wurtzite phase [35]; (ii) bands at approximately  $332 \text{ cm}^{-1}$  and several common low-frequency features should be assigned to the second-order Raman spectrum arising from zone boundary phonons  $3E_{2H}-E_{2L}$ ; (iii) at  $530 \text{ cm}^{-1}$ , a very weak band from the  $E_1$  (LO) mode of ZnO associated with oxygen deficiency [36]. Its intensity depends upon the crystallinity,

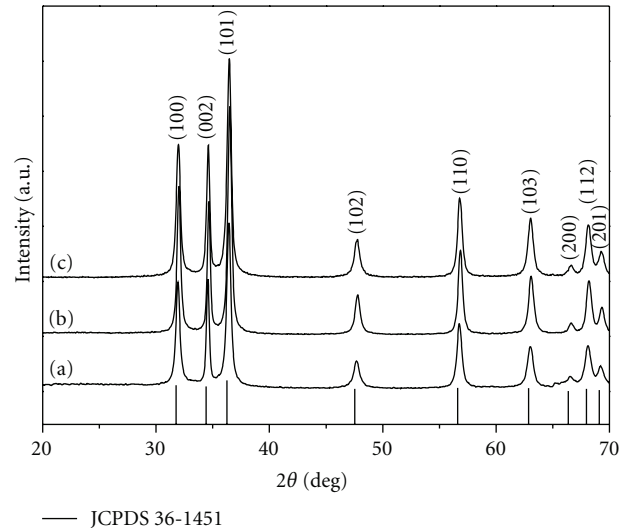


FIGURE 1: XRD patterns of the ZnO sample obtained by (a) conventional water bath heating, (b) the MH method for 2 min, and (c) the MH method for 8 min.

preparation method and crystal orientation. Figure 2 shows Raman spectra of ZnO powders obtained. The asymmetric band at  $378 \text{ cm}^{-1}$  ( $A_{1T}$  mode) related to the structural order-disorder in the lattice [37] is covered by broad band characteristic of a Zn–O bond at  $437 \text{ cm}^{-1}$ .

Well-crystallized zinc compounds with different morphologies can be obtained by several synthesis methods by using urea (see Table 1). Precursors, the concentration of urea, the synthesis method and the reaction time are important factors influencing the structural evolution and the morphology of the products. The weak basicity of the solution gives rise to a zinc carbonate species product (Table 1). The use of MH crystallization facilitates the direct preparation of pure oxide powders in less time with desired particle sizes and shapes from the control parameters such as solution pH, reaction temperature, reaction time, solute concentration and the type of solvent [38–40].

Hydrolysis characteristics of urea are well known in  $\text{H}_2\text{O}$  over  $293\text{--}373 \text{ K}$  at 1 bar [41]. Urea is highly soluble in water, and its controlled hydrolysis in aqueous solutions can yield ammonia and carbon dioxide. In the crystal growth process, first ZnO tiny crystalline nuclei were formed, and nanoparticles of this oxide were precipitated by an increase in pH due to  $\text{NH}_4^+$  ions generated from  $\text{NH}_3$  which resulted from urea decomposition when the temperature rose. The  $\text{NH}_4^+$  ion formation is controlled by ammonia in water, and the hydrolysis of urea leads to a rise in the pH. The urea hydrolysis progresses slowly, and the basic solution undergoes supersaturation of the zinc hydroxide species [42]. Thus, the formation of ZnO occurs by a nucleation process and the preferred growth direction of the crystal.

During the MH process, the urea is readily hydrolyzed; its hydrolysis is also accompanied by the formation of gas molecules and an increase in the pressure in the system which is expected to perturb nanocrystalline growth and thereby

TABLE 1: Zinc species obtained by different synthesis method using urea as a precursor.

Synthesis method	Product 1	Temperature/time	Product 2	Morphology/size	Reference
Precipitation	$Zn_5(OH)_6(CO_3)_2 + ZnO$	4 h of synthesis	ZnO	Bipods/3.1–7.9 $\mu m$	[3]
Precipitation	$[Zn(OH)_2(H_2O)_2]$	1000°C/2 h	ZnO	Hexagonal plates/35–45 $\mu m$	[6]
Sol-gel	$Zn_5(OH)_6(CO_3)_2$	500°C–900°C/2 h	ZnO	Spherical particles/20 nm	[28]
Conventional hydrothermal	white powder	550°C/4 h	ZnO	Column-, rosette-fiber-like/0.5–10 $\mu m$	[29]
Microwave-induced combustion technique	ZnO	—	—	Flowers-like/2–5 $\mu m$	[30]
Refluxing route	ZnO	—	—	Rods-likes/30–40 nm (diameter) and 500–700 nm (length)	[31]
Conventional hydrothermal	$Zn_5(OH)_6(CO_3)_2$	500°C/1 h	ZnO	Spherical particles/25 nm	[32]
Conventional hydrothermal	$Zn_4(OH)_6CO_3 \cdot H_2O$	400°C/2 h	ZnO	Flakes-like/0.65–1.5 $\mu m$	[33]
Conventional hydrothermal	$Zn_5(OH)_6(CO_3)_2$	600°C	ZnO	Flakes-like/10–20 nm	[11]
Solvothermal	$ZnOCO_3 + ZnO$	180°C/24 h	ZnO	Spherical particles/50–300 nm	[23]
Urea aqueous solution process	$Zn_5(OH)_6(CO_3)_2$	600°C/30 min	ZnO	Spherical chrysanthemums/2–6 $\mu m$	[34]
Conventional water bath heating	ZnO	—	—	Irregular nanoparticles	This work
Microwave-assisted hydrothermal	ZnO	—	—	Spheres-like/85 nm	This work

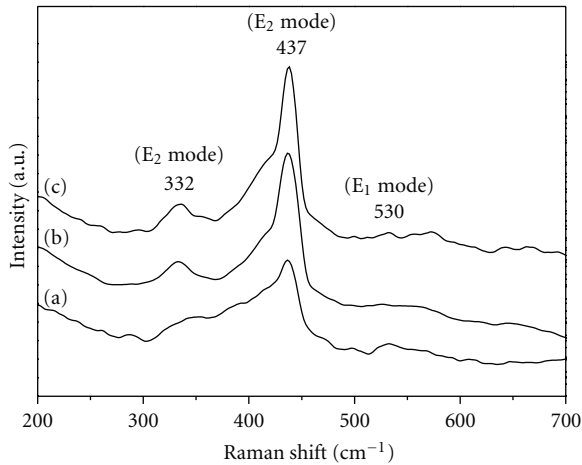


FIGURE 2: Raman spectra of ZnO powders prepared by (a) conventional water bath heating, (b) the MH method for 2 min, and (c) the MH method for 8 min.

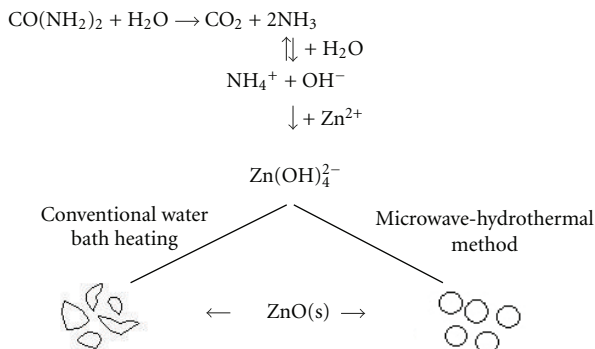


FIGURE 3: Schematic representation of ZnO formation.

TABLE 2: Fitting parameters of five Gaussian peaks.

Peak center (eV)	1.76	1.95	2.15	2.36	2.61
Conventional water bath heating (area %)	11.1	29.0	34.5	19.0	6.4
MH for 2 min (area %)	10.1	26.1	31.2	24.1	8.5
MH for 8 min (area %)	9.2	29.9	33.5	20.8	6.5

results in morphological changes. This process may accelerate the reaction between the synthesis precursors which leads to anisotropic crystal growth and the crystallization of oxide under mild temperature conditions and reaction times. A schematic representation of ZnO nanostructure formation is shown in Figure 3.

The morphology of ZnO powders was investigated using FE-SEM (see Figure 4). These images reveal that samples prepared without the MH process had an irregular shape and were not uniform in size, whereas spherical and uniform particles were observed for samples prepared using the MH method. The MH method contributes significantly to ZnO production with homogeneous shapes after short processing times.

Diffusivity in the medium and interface mobility could be enhanced using the MH process which contributes significantly to ZnO production with homogeneous shapes after short processing times. Nanosized structures were formed by this method, and different average particle distributions were obtained after treatment under hydrothermal conditions (see inset in Figures 4(b) and 4(c)). Average particle diameters were 90 nm and 85 nm for samples treated by the MH process for 2 and 8 min, respectively.

Disordered structures in solids cause degeneracy and destabilization in the localized states of the atoms which act

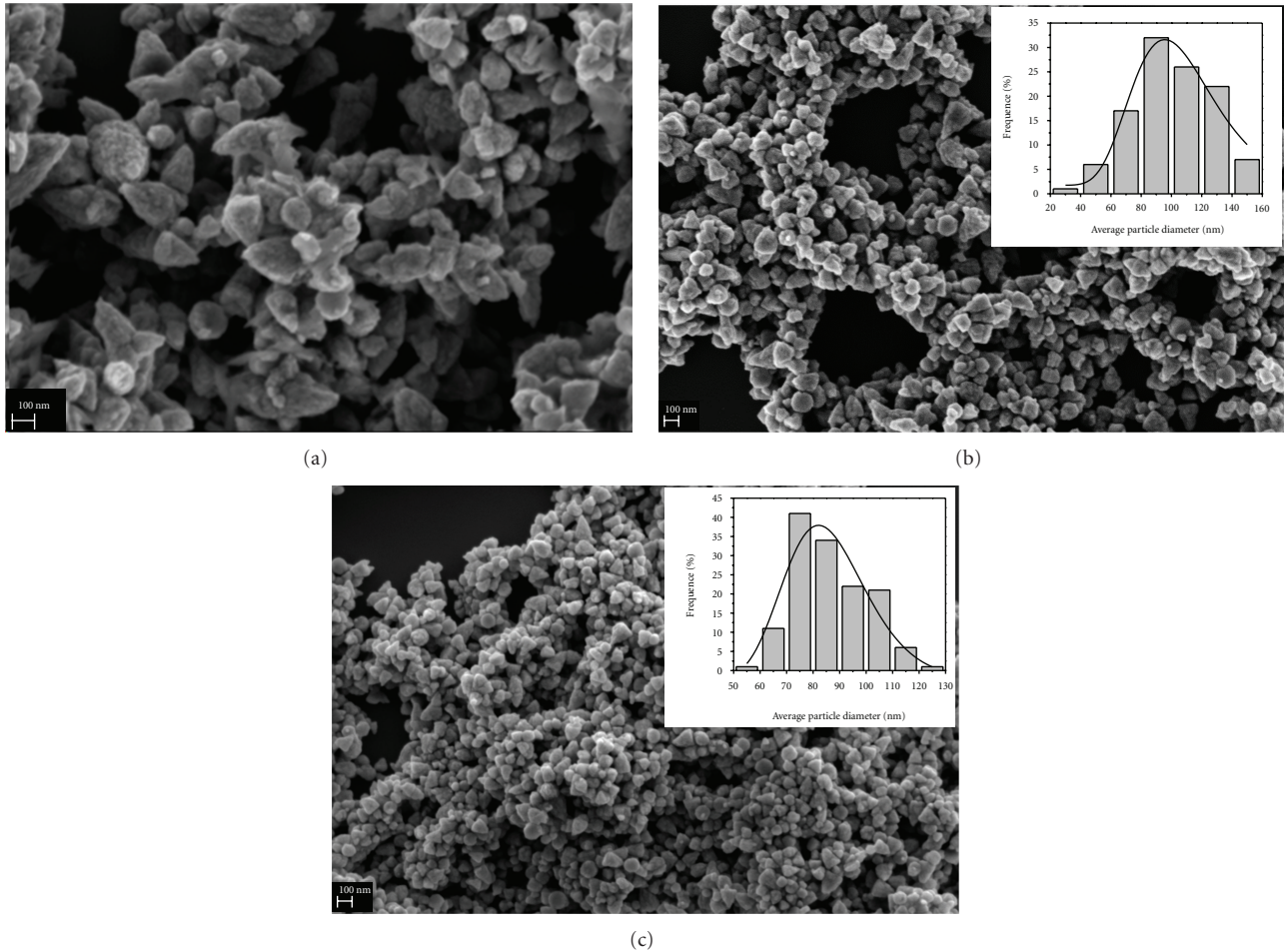


FIGURE 4: FE-SEM images of ZnO powders prepared using (a) conventional water bath heating, (b) the MH method for 2 min (average distribution of particles is inserted), and (c) the MH method for 8 min (average distribution of particles is inserted).

as electron-hole pairs and support broadband PL phenomena. PL spectra recorded at room temperature are illustrated in Figure 5(a).

Theoretical results verify that a symmetry breaking process in the structure of various semiconductors associated with order-disorder effects is a necessary condition for intermediate levels in the forbidden band gap [43–45]. These structural changes can be related to the charge polarization in different ranges that are (at the very least) manifestations of quantum confinement when they occur at short and intermediate ranges independent of the particle size. The main reason for quantum confinement to occur is the formation of discrete levels in the band gap which is not possible with as a periodic crystal defect (dispersion interaction) [46]. The formation of isolated energy levels (quantum confinement) and  $[\text{ZnO}_3 \cdot \text{V}_0^*]$  clusters leads to a substantial recombination between photoexcited electrons and holes during the excitation process. Probably the  $[\text{ZnO}_4]^x - [\text{ZnO}_3 \cdot \text{V}_0^x]$  clusters are activated during the excitation process which changes their symmetry in progressing from singlet or triplet states as demonstrated for the perovskite

structure [47]. These defects induce new energies in the band gap which can be attributed to zinc-oxygen vacancy centers. The structural and electronic reconstructions of all possible combinations of clusters in a crystal are essential to understand the cluster-to-cluster charge transfer process and even the PL phenomenon.

PL curves were decomposed into five components using the Gaussian method and the Peak Fit program: a red component (1.76 eV), a yellow component (1.95 eV), two green components (2.15 and 2.36 eV), and a blue component (2.61 eV). These emissions arise from a radiative recombination between electrons and holes trapped in the gap states. Figures 5(b) to 5(d) illustrate decomposition data, and Table 2 lists the areas under each curve of the respective transitions. The percentage was obtained by dividing the area of each decomposed PL curve by the total PL area. Each color represents a different type of electronic transition and can be linked to a specific structural arrangement. The high PL intensity displayed by the sample obtained for 2 min under MH conditions seems to indicate that this material must

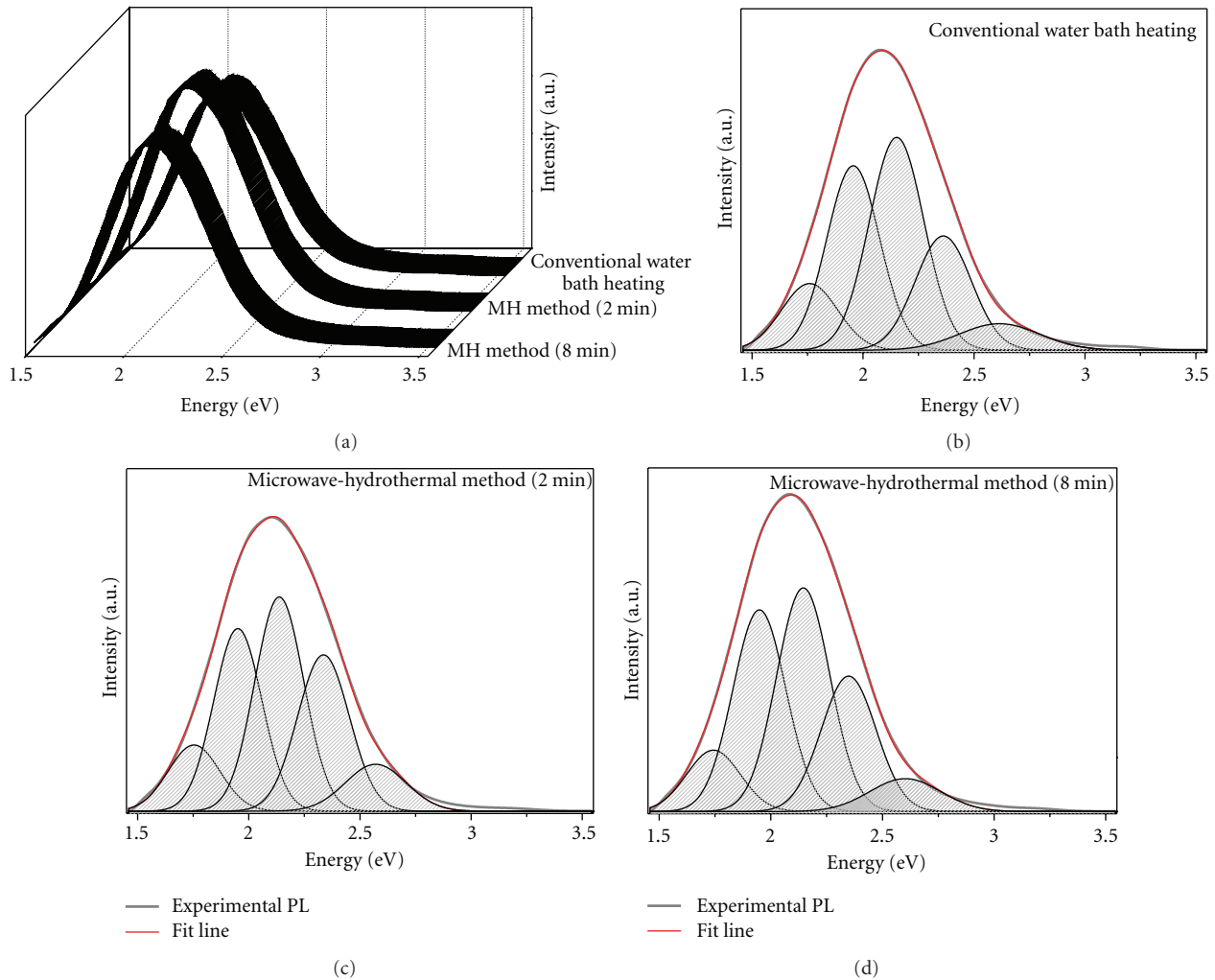


FIGURE 5: (a) PL spectra at room temperature of ZnO powders; deconvolution results of ZnO samples obtained by (b) conventional water bath heating, (c) the MH method for 2 min, and (d) the MH method for 8 min.

possess an optimum structural order-disorder degree for PL to occur.

#### 4. Conclusions

The MH process affects the growth process of ZnO nanostructures from an aqueous solution of zinc acetate and urea which leads to the rapid and uniform growth of particles. The PL emission of semiconductors is an important property because it can provide information on defects and relaxation pathways of excited states depending upon the preparation techniques which can generate different structural defects.

#### Acknowledgments

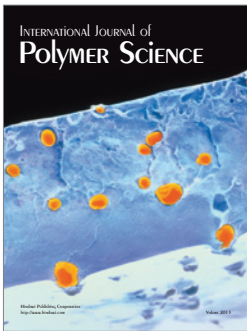
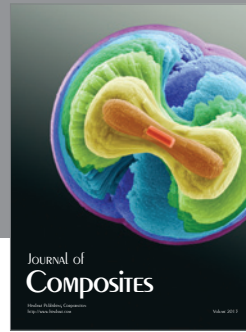
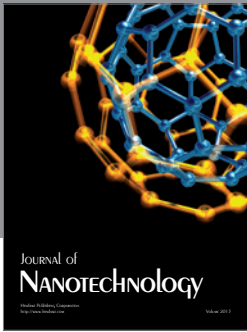
The authors gratefully acknowledge the agencies FAPEMIG, CNPq, CAPES, and FAPESP.

#### References

- [1] Y. Huang, X. Duan, Q. Wei, and C. M. Lieber, "Directed assembly of one-dimensional nanostructures into functional networks," *Science*, vol. 291, no. 5504, pp. 630–633, 2001.
- [2] Q. X. Zhao, M. Willander, R. E. Morjan, Q. H. Hu, and E. E. B. Campbell, "Optical recombination of ZnO nanowires grown on sapphire and Si substrates," *Applied Physics Letters*, vol. 83, no. 1, pp. 165–167, 2003.
- [3] M. Bitenc and Z. Crnjak Orel, "Synthesis and characterization of crystalline hexagonal bipods of zinc oxide," *Materials Research Bulletin*, vol. 44, no. 2, pp. 381–387, 2009.
- [4] A. M. Peiró, P. Ravirajan, K. Govender et al., "Hybrid polymer/metal oxide solar cells based on ZnO columnar structures," *Journal of Materials Chemistry*, vol. 16, no. 21, pp. 2088–2096, 2006.
- [5] C. K. Srikanth and P. Jeevanandam, "Effect of anion on the homogeneous precipitation of precursors and their thermal decomposition to zinc oxide," *Journal of Alloys and Compounds*, vol. 486, no. 1-2, pp. 677–684, 2009.

- [6] K. Ada, M. Goekgoez, M. Oenal, and Y. Sankaya, "Preparation and characterization of a ZnO powder with the hexagonal plate particles," *Powder Technology*, vol. 181, no. 3, pp. 285–291, 2008.
- [7] C. Cheng, B. Liu, H. Yang et al., "Hierarchical assembly of ZnO nanostructures on SnO<sub>2</sub> backbone nanowires: low-temperature hydrothermal preparation and optical properties," *ACS Nano*, vol. 3, no. 10, pp. 3069–3076, 2009.
- [8] S. Baruah and J. Dutta, "Hydrothermal growth of ZnO nanostructures," *Science and Technology of Advanced Materials*, vol. 10, no. 1, Article ID 013001, 2009.
- [9] S. D. G. Ram, M. A. Kulandainathan, and G. Ravi, "On the study of pH effects in the microwave enhanced rapid synthesis of nano-ZnO," *Applied Physics A*, vol. 99, no. 1, pp. 197–203, 2010.
- [10] S. A. M. Lima, M. Cremona, M. R. Davolos, C. Legnani, and W. G. Quirino, "Electroluminescence of zinc oxide thin-films prepared via polymeric precursor and via sol-gel methods," *Thin Solid Films*, vol. 516, no. 2–4, pp. 165–169, 2007.
- [11] S. Music, S. Popovic, M. Maljkovic, and E. Dragecic, "Influence of synthesis procedure on the formation and properties of zinc oxide," *Journal of Alloys and Compounds*, vol. 347, no. 1–2, pp. 324–332, 2002.
- [12] A. M. Peiro, C. Domingo, J. Peral et al., "Nanostructured zinc oxide films grown from microwave activated aqueous solutions," *Thin Solid Films*, vol. 483, no. 1–2, pp. 79–83, 2005.
- [13] J. Jiang, Y. Li, S. Tan, and Z. Huang, "Synthesis of zinc oxide nanotetrapods by a novel fast microemulsion-based hydrothermal method," *Materials Letters*, vol. 64, no. 20, pp. 2191–2193, 2010.
- [14] M. Mo, J. C. Yu, L. Zhang, and S. K. A. Li, "Self-assembly of ZnO nanorods and nanosheets into hollow microhemispheres and microspheres," *Advanced Materials*, vol. 17, no. 6, pp. 756–760, 2005.
- [15] A. Wei, X. W. Sun, C. X. Xu et al., "Growth mechanism of tubular ZnO formed in aqueous solution," *Nanotechnology*, vol. 17, no. 6, pp. 1740–1744, 2006.
- [16] D. R. Chen, X. Jiao, and G. Cheng, "Hydrothermal synthesis of zinc oxide powders with different morphologies," *Solid State Communications*, vol. 113, no. 6, pp. 363–366, 2000.
- [17] C. H. Lu and C. H. Yeh, "Influence of hydrothermal conditions on the morphology and particle size of zinc oxide powder," *Ceramics International*, vol. 26, no. 4, pp. 351–357, 2000.
- [18] A. P. de Moura, R. C. Lima, M. L. Moreira et al., "ZnO architectures synthesized by a microwave-assisted hydrothermal method and their photoluminescence properties," *Solid State Ionics*, vol. 181, no. 15–16, pp. 775–780, 2010.
- [19] Y.-C. Chen and S. L. Lo, "Effects of operational conditions of microwave-assisted synthesis on morphology and photocatalytic capability of zinc oxide," *Chemical Engineering Journal*, vol. 170, no. 2–3, pp. 411–418, 2011.
- [20] L. N. Dem'yanets, V. V. Artemov, L. E. Li, Y. M. Mininon, and T. G. Uvarova, "Zinc oxide hollow microstructures and nanostructures formed under hydrothermal conditions," *Crystallography Reports*, vol. 53, no. 5, pp. 888–893, 2008.
- [21] Y. P. Fang, X. Wen, S. Yang et al., "Hydrothermal synthesis and optical properties of ZnO nanostructured films directly grown from/on zinc substrates," *Journal of Sol-Gel Science and Technology*, vol. 36, no. 2, pp. 227–234, 2005.
- [22] C. G. Kim, K. Sung, T. M. Chung, D. Y. Jung, and Y. Kim, "Monodispersed ZnO nanoparticles from a single molecular precursor," *Chemical Communications*, vol. 9, no. 16, pp. 2068–2069, 2003.
- [23] C. L. Wang, E. Wang, E. Shen et al., "Growth of ZnO nanoparticles from nanowhisker precursor with a simple solvothermal route," *Materials Research Bulletin*, vol. 41, no. 12, pp. 2298–2302, 2006.
- [24] E. Savary, S. Marinel, H. Colder, C. Harnois, F. X. Lefevre, and R. Retoux, "Microwave sintering of nano-sized ZnO synthesized by a liquid route," *Powder Technology*, vol. 208, no. 2, pp. 521–525, 2011.
- [25] M. L. Dos Santos, R. C. Lima, C. S. Riccardi et al., "Preparation and characterization of ceria nanospheres by microwave-hydrothermal method," *Materials Letters*, vol. 62, no. 30, pp. 4509–4511, 2008.
- [26] L. S. Cavalcante, J. C. Sczancoski, J. W. M. Espinosa, J. A. Varela, P. S. Pizani, and E. Longo, "Photoluminescent behavior of BaWO<sub>4</sub> powders processed in microwave-hydrothermal," *Journal of Alloys and Compounds*, vol. 474, no. 1–2, pp. 195–200, 2009.
- [27] J. F. Huang, C. Xia, L. Cao, and X. Zeng, "Facile microwave hydrothermal synthesis of zinc oxide one-dimensional nanostructure with three-dimensional morphology," *Materials Science and Engineering B*, vol. 150, no. 3, pp. 187–193, 2008.
- [28] R. Wahab, S. G. Ansari, Y. S. Kim, M. A. Dar, and H. S. Shin, "Synthesis and characterization of hydrozincite and its conversion into zinc oxide nanoparticles," *Journal of Alloys and Compounds*, vol. 461, no. 1–2, pp. 66–71, 2008.
- [29] G. F. Zou, D. Yu, D. Wang et al., "Controlled synthesis of ZNO nanocrystals with column-, rosette- and fiber-like morphologies and their photoluminescence property," *Materials Chemistry and Physics*, vol. 88, no. 1, pp. 150–154, 2004.
- [30] Y. A. Cao, B. Liu, R. Huang, Z. Xia, and S. Ge, "Flash synthesis of flower-like ZnO nanostructures by microwave-induced combustion process," *Materials Letters*, vol. 65, no. 2, pp. 160–163, 2011.
- [31] J. W. Zhang, W. Wang, P. Zhu, J. Chen, Z. Zhang, and Z. Wu, "Synthesis of small diameter ZnO nanorods via refluxing route in alcohol-water mixing solution containing zinc salt and urea," *Materials Letters*, vol. 61, no. 2, pp. 592–594, 2007.
- [32] S.-H. Hu, Y. C. Chen, C. C. Hwang, C. H. Peng, and D. C. Gong, "Analysis of growth parameters for hydrothermal synthesis of ZnO nanoparticles through a statistical experimental design method," *Journal of Materials Science*, vol. 45, no. 19, pp. 5309–5317, 2010.
- [33] L. L. Wu, Y. Wu, and Y. Lü, "Self-assembly of small ZnO nanoparticles toward flake-like single crystals," *Materials Research Bulletin*, vol. 41, no. 1, pp. 128–133, 2006.
- [34] M. Bitenc, M. Marinšek, and Z. Crnjak Orel, "Preparation and characterization of zinc hydroxide carbonate and porous zinc oxide particles," *Journal of the European Ceramic Society*, vol. 28, no. 15, pp. 2915–2921, 2008.
- [35] C. Li, Y. Lv, L. Guo, H. Xu, X. Ai, and J. Zhang, "Raman and excitonic photoluminescence characterizations of ZnO star-shaped nanocrystals," *Journal of Luminescence*, vol. 122–123, no. 1–2, pp. 415–417, 2007.
- [36] C. F. Windisch Jr, G. J. Exarhos, C. Yao, and L. Q. Wang, "Raman study of the influence of hydrogen on defects in ZnO," *Journal of Applied Physics*, vol. 101, no. 12, Article ID 123711, 2007.
- [37] Z. W. Dong, C. F. Zhang, H. Deng, G. J. You, and S. X. Qian, "Raman spectra of single micrometer-sized tubular ZnO," *Materials Chemistry and Physics*, vol. 99, no. 1, pp. 160–163, 2006.
- [38] J. S. Lee and S. C. Choi, "Crystallization behavior of nano-ceria powders by hydrothermal synthesis using a mixture of H<sub>2</sub>O<sub>2</sub>

- and  $\text{NH}_4\text{OH}$ ,” *Materials Letters*, vol. 58, no. 3-4, pp. 390–393, 2004.
- [39] S. Komarneni, Q. H. Li, and R. Roy, “Microwave-hydrothermal processing for synthesis of layered and network phosphates,” *Journal of Materials Chemistry*, vol. 4, no. 12, pp. 1903–1906, 1994.
- [40] S. Komarneni, R. Pidugu, Q. H. Li, and R. Roy, “Microwave-hydrothermal processing of metal powders,” *Journal of Materials Research*, vol. 10, no. 7, pp. 1687–1692, 1995.
- [41] M. L. Kieke, J. W. Schoppelrei, and T. B. Brill, “Spectroscopy of hydrothermal reactions. 1. The  $\text{CO}_2$ - $\text{H}_2\text{O}$  system and kinetics of urea decomposition in an FTIR spectroscopy flow reactor cell operable to 725 K and 335 bar,” *Journal of Physical Chemistry*, vol. 100, no. 18, pp. 7455–7462, 1996.
- [42] K. Kakiuchi, E. Hosono, T. Kimura, H. Imai, and S. Fujihara, “Fabrication of mesoporous ZnO nanosheets from precursor templates grown in aqueous solutions,” *Journal of Sol-Gel Science and Technology*, vol. 39, no. 1, pp. 63–72, 2006.
- [43] E. Longo, E. Orhan, F. M. Pontes et al., “Density functional theory calculation of the electronic structure of  $\text{Ba}_{0.5}\text{Sr}_{0.5}\text{TiO}_3$ : photoluminescent properties and structural disorder,” *Physical Review B*, vol. 69, no. 12, pp. 125115–125117, 2004.
- [44] V. M. Longo, E. Orhan, L. S. Cavalcante et al., “Understanding the origin of photoluminescence in disordered  $\text{Ca}_{0.60}\text{Sr}_{0.40}\text{WO}_4$ : an experimental and first-principles study,” *Chemical Physics*, vol. 334, no. 1–3, pp. 180–188, 2007.
- [45] R. C. Lima, L. R. Macario, J. W. M. Espinosa et al., “Toward an understanding of intermediate- and short-range defects in ZnO single crystals. A combined experimental and theoretical study,” *Journal of Physical Chemistry A*, vol. 112, no. 38, pp. 8970–8978, 2008.
- [46] R. C. Lima, J. Andres, J. R. Sambrano et al., *Photoluminescence: Applications, Types and Efficacy: An Overview on the Photoluminescence Emission in ZnO Single Crystal: A Joint Experimental and Theoretical Analysis*, Nova Science Publishers, New York, NY, USA, 2012.
- [47] L. Gracia, J. Andrés, V. M. Longo, J. A. Varela, and E. Longo, “A theoretical study on the photoluminescence of  $\text{SrTiO}_3$ ,” *Chemical Physics Letters*, vol. 493, no. 1–3, pp. 141–146, 2010.



**Hindawi**

Submit your manuscripts at  
<http://www.hindawi.com>

